Food Hydrocolloids

A Millifluidic-assisted ionic gelation technique for encapsulation of probiotics in double-layered polysaccharide structure

--Manuscript Draft--

Manuscript Number:	FOODHYD-D-21-03408
Article Type:	Research paper
Keywords:	Millifluidic; Probiotics; Ionic gelation; Double-layered; In vitro digestion; Viability
Corresponding Author:	Behrouz Ghorani Research Institute of Food Science and Technology Mashhad, IRAN, ISLAMIC REPUBLIC OF
First Author:	Atefeh Farahmand, PhD Student
Order of Authors:	Atefeh Farahmand, PhD Student
	Behrouz Ghorani
	Bahareh Emadzadeh, PhD
	Mahboobe Sarabi-Jamab, PhD
	Maryam Emadzadeh, PhD
	Atena Modiri, PhD Student
	Nick Tucker, PhD
Abstract:	A unique double-layered probiotic delivery system based on a millifluidic/direct gelation method of encapsulation has been investigated. The effects of variation of alginate concentration (20-30 g/l), flow rates of alginate (0.8-1.2 ml/min), and water/oil (W/O) emulsion (0.5-0.7 ml/min) on emulsion encapsulation efficiency (EE), size, and sphericity (SF) of core-shell millicapsules were examined using a central composite design to optimize a delivery system for the encapsulated Bifidobacterium animalis subsp. lactis and Lactobacillus plantarum. The optimized calcium-alginate millicapsule was spherical (0.97± 0.01 SF), with an average diameter of 4.49± 0.19 mm, and an emulsion encapsulation efficiency of 98.17± 0.5%. Two probiotic strains were encapsulated separately in W/O emulsion as a core of the millicapsule. After coating with chitosan, the encapsulation yield of the bacteria, survival rates under simulated gastrointestinal (GI) conditions, and viability during storage were determined. Survival efficiency values of B. animalis subsp. lactis and L. plantarum after millifluidic encapsulation were found to be 92.33 and 90.81%, respectively. Cell viability of probiotics embedded in the millicapsule after passing through the GI system was improved (7.5 log CFU ml-1 for both strains). Although the viability of the encapsulated probiotics stored at -18 °C for six months significantly decreased ($p< 0.05$), the number of live cells was approximately in accordance with the standard definition of long-term probiotic survival (6 log CFU g-1).
Suggested Reviewers:	Hans Tromp, PhD Researcher, NIZO Food Research BV Hans.Tromp@nizo.com Expert in encapsulation of probiotic & polysaccharides/ ionic gelation
	Asgar Farahnaky, PhD Academic Staff, RMIT University asgar.farahnaky@rmit.edu.au Expert in ionic gelation/ delivery systems and polysaccharides
	Amparo López Rubio, PhD Spanish Scientific Research Council: Consejo Superior de Investigaciones Cientificas amparo.lopez@iata.csic.es Expert in Encapsulation of Probiotics
	Ali Marefati, PhD Researcher, Aarhus University: Aarhus Universitet am@food.au.dk

	Expert in Emulsion systems & Encapsulation of Probiotics

Dear Prof. P.A. Williams,

Editor-in-Chief of Food Hydrocolloids,

I wish to submit a new research manuscript entitled ‘’ **A Millifluidic-assisted ionic gelation technique for encapsulation of probiotics in double-layered polysaccharide structure**’’ for consideration by the journal of Food Hydrocolloids.

This is the first report of using two techniques (Millifluidic and ionic gelation) simultaneously as the ‘’double-layered strategy platform’’ for encapsulation of probiotic strains.

The ‘’millifluidic’’ technique could be considered as a ‘’novel approach’’ for ‘’encapsulation’’ of ‘’bioactive compounds ‘’ and has a promising perspective in the field of food engineering or pharmaceutical science (drug delivery systems). To the best of our knowledge, despite of the advantages of millifluidic technique as an encapsulation process, no study has optimized this method for the encapsulation of probiotic bacteria. Therefore, in this study we aim to optimize the millifluidic technique for the encapsulation of two probiotic bacteria species, *Bifidobacterium animalis* subsp. lactis and *Lactobacillus plantarum*, separately, into optimal W/O emulsion-filled millicapsules and to assess survival rates during storage and the viability of the encapsulated probiotics under simulated GI conditions.

Accordingly, the utility of the millifluidic encapsulation method paves the way for fabrication of a unique carrier for probiotic bacteria. Furthermore, <u>encapsulation of lipophilic compounds in the oil part and hydrophilic compounds in the water part of emulsion loaded in millicapsules can be exploited co-encapsulation in various domains.</u>

This project has successfully been accomplished at Department of Food Nanotechnology, Research Institute of Food Science & Technology (RIFST) and Mashhad University of Medical Science, (IRAN). This novel work has also been internationally extended and professionally supervised by my colleague Dr. Nick Tucker, from University of Lincoln (UK).

I would be most grateful if we could receive the invaluable comments of the reviewers and have a chance to publish our paper in the high prestigious journal of Food Hydrocolloids.

Thank you very much indeed for your consideration of this manuscript.

Respectfully yours,

Behrouz Ghorani

12/15/2021

Dr.Behrouz Ghorani
(Corresponding author)

Team Leader of Electrospinning Research Group
Department of Food Nanotechnology
Research Institute of Food Science &Technology (RIFST)
Km 12 Mashhad-Quchan Highway
Mashhad, Khorasan Razavi, IRAN
P.O.Box : 91895/157/356
Tel: +98-51-35425386
Cell: +98-915-317-3173
Fax: +98-51-35425406
Email: behrooz.ghorani@gmail.com or b.ghorani@rifst.ac.ir

Highlights

- A millifluidic /direct gelation method was applied for encapsulation of probiotics.
- The central composite design was used for the optimization of the gelation process.
- The optimal emulsion-filled millicapsules had monodispersed spherical shapes.
- The survival efficiency of two encapsulated probiotic strains was higher than 90%.
- After 6 month storage at -18°C, the number of live cells still met the standards.

Graphical Abstract

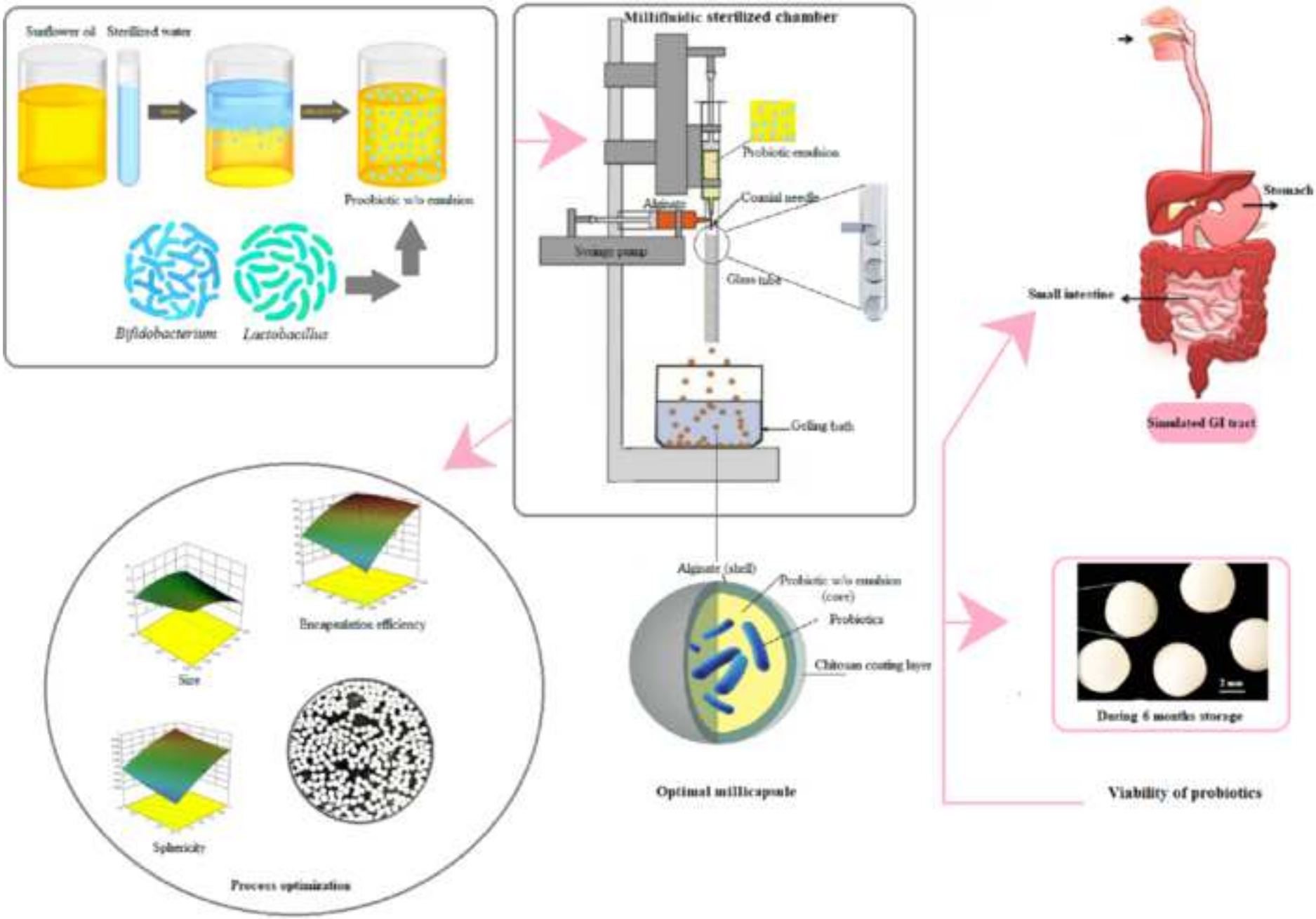

A Millifluidic-assisted ionic gelation technique for encapsulation of probiotics in double-layered polysaccharide structure

Atefeh Farahmand[1], Behrouz Ghorani[*1], Bahareh Emadzadeh[1], Mahboobe Sarabi-Jamab[2], Maryam Emadzadeh[3], Atena Modiri[1], Nick Tucker[4]

[1] Department of Food Nanotechnology, Research Institute of Food Science and Technology, km 12 Mashhad-Quchan Highway, Mashhad, Iran

[2] Department of Food Microbiology, Research Institute of Food Science and Technology, km 12 Mashhad-Quchan Highway, Mashhad, Iran

[3] Clinical Research Development Unit, Ghaem Hospital, Mashhad University of Medical Sciences, Mashhad, Iran

[4] University of Lincoln, School of Engineering, Brayford Pool, Lincoln, LN6 7TS, United Kingdom (UK)

*Corresponding author: Dr. Behrouz Ghorani

Department of Food Nanotechnology

Research Institute of Food Science & Technology (RIFST), km 12 Mashhad-Quchan Highway, Khorasan Razavi, Mashhad, Iran, P.O. Box: 91895-157-356

E-mail: b.ghorani@rifst.ac.ir

Abstract

A unique double-layered probiotic delivery system based on a millifluidic/direct gelation method of encapsulation has been investigated. The effects of variation of alginate concentration (20-30 g/l), flow rates of alginate (0.8-1.2 ml/min), and water/oil (W/O) emulsion (0.5-0.7 ml/min) on emulsion encapsulation efficiency (EE), size, and sphericity (SF) of core-shell millicapsules were examined using a central composite design to optimize a delivery system for the encapsulated *Bifidobacterium animalis* subsp. *lactis* and *Lactobacillus plantarum*. The optimized calcium-alginate millicapsule was spherical (0.97± 0.01 SF), with an average diameter of 4.49± 0.19 mm, and an emulsion encapsulation efficiency of 98.17± 0.5%. Two probiotic strains were encapsulated separately in W/O emulsion as a core of the millicapsule. After coating with chitosan, the encapsulation yield of the bacteria, survival rates under simulated gastrointestinal (GI) conditions, and viability during storage were determined. Survival efficiency values of *B. animalis* subsp. *lactis* and *L. plantarum* after millifluidic encapsulation were found to be 92.33 and 90.81%, respectively. Cell viability of probiotics embedded in the millicapsule after passing through the GI system was improved (7.5 log CFU ml^{-1} for both strains). Although the viability of the encapsulated probiotics stored at -18 °C for six months significantly decreased ($p < 0.05$), the number of live cells was approximately in accordance with the standard definition of long-term probiotic survival (6 log CFU g^{-1}).

Keywords: Millifluidic, Probiotics, Ionic gelation, Double-layered, In vitro digestion, Viability

1. Introduction

Probiotics are defined as living microorganisms that confer beneficial health effects on the host when administered in adequate amounts. Some positive effects of probiotics are the production of pathogen inhibitory substances, the prevention of adhesion of certain bacterial cells, toxin degradation, beneficial modulation of the gastrointestinal (GI) microbial flora, and a general enhancement of the immune system (Khaneghah, et al., 2020; Zhijing Liu, et al., 2020). To accomplish these beneficial functions, the probiotics must first survive being subject to variations in pH, oxidative conditions, and high temperature whilst processed into an edible form and then the harsh digestive conditions of the GI tract (acidity, bile salts, digestive enzymes), to reach the intestine in an appropriate quantity (Holkem, et al., 2016; Li, et al., 2019). Microencapsulation is an established technique to allow the survival of probiotics in food processing and formulations, and once through the GI tract, to promote their ability to colonize the mucosal surfaces (Anselmo, McHugh, Webster, Langer, & Jaklenec, 2016). However, very low or high temperatures, and/or organic agents that are part of common probiotic encapsulation techniques such as spray drying, freeze and fluid bed drying, and coacervation, lead to a considerable reduction in bacterial viability (Zaeim, et al., 2020), therefore alternative methods for drying and encapsulation of probiotics are desirable (Alehosseini, Sarabi-Jamab, Ghorani, & Kadkhodaee, 2019).

Multilayer delivery systems have been proposed to improve the survival rate of encapsulated probiotics. Examples are the encapsulation of *Lactobacillus paracasei BGP-1* in alginate/shellac by co-extrusion (Silva, et al., 2016), moist-heat-resistant multilayered microcapsules for encapsulation of *Lactobacillus acidophilus* (Pitigraisorn, Srichaisupakit, Wongpadungkiat, & Wongsasulak, 2017), encapsulation of *Lactobacillus acidophilus* in zein-

alginate core-shell microcapsules by electrospraying (Laelorspoen, Wongsasulak, Yoovidhya, & Devahastin, 2014) and the encapsulation of *Lactobacillus reuteri* in water/oil/water (W/O/W) double emulsions (Marefati, Pitsiladis, Oscarsson, Ilestam, & Bergenståhl, 2021). It is proposed that a double-layer delivery system could be developed using millifluidic encapsulation: this is a fast, straight forward, and cost effect manufacturing method that does not require toxic chemicals (Martins, Poncelet, Marquis, Davy, & Renard, 2017; Nativel, et al., 2018). Compared with conventional techniques such as extrusion or emulsification which generally have poor control of capsule diameter, the millifluidic method produces highly monodispersed droplets through precise control of the flow of both the dispersed and continuous phases. The hydrophobic core (an emulsion containing the probiotics) exists as a dispersed phase and the hydrophilic shell (sodium alginate solution) is a continuous phase and these are extruded into a tube. The double-layered droplets are formed by the shear forces between the two phases. Due to this opposition of forces the droplets fall into a gelling bath, and chemical interactions between the polymer chains and calcium ions produce a core-shell delivery system. Alginate as an anionic linear polysaccharide is degraded at a very low pH, therefore, the combination of this polymer with certain polycationic polymers such as chitosan leads to the formation of strong electrostatic repulsive forces between the amine and acid residues (Nualkaekul, Lenton, Cook, Khutoryanskiy, & Charalampopoulos, 2012). The millifluidic technique has been used for the production of emulsion oil-loaded capsules. According to Martins, et al. (2017), encapsulation of a W/O emulsion into capsules with the sizes ranging from 140 µm to 1.4 mm was successfully achieved using the millifluidic/inverse gelation mechanism. Pereda, Poncelet, and Renard (2019) studied the influence of curing time and storage conditions on the physicochemical characteristics of the core-shell millicapsules produced by the

millifluidic/inverse gelation technique. Geometric, instrumental, and phases features of millifluidic/ dripping process were assessed for sunflower oil-loaded millicapsules (Farahmand, Emadzadeh, Ghorani, & Poncelet, 2021) who also examined flow pattern, droplet formation mechanism, and forces experienced by droplets inside the millifluidic device.

Recently, the millifluidic process has been extended to the microfluidic scale, which has been used for the cultivation of individual bacteria inside microfluidic double-layered emulsion droplets (Yoha, Nida, Dutta, Moses, & Anandharamakrishnan, 2021). A W/O emulsion of okara oil and block-copolymers of poly (acrylic acid) and Pluronics® has been used in a microfluidic device for the encapsulation of *Lactobacillus plantarum* (Quintana, et al., 2021).

To the best of our knowledge, despite of the advantages of millifluidic technique as an encapsulation process, no study has optimized this method for the encapsulation of probiotic bacteria. Therefore, in this study we aim to optimize the millifluidic technique for the encapsulation of two probiotic bacteria species, *Bifidobacterium animalis* subsp. *lactis* and *Lactobacillus plantarum*, separately, into optimal Ca-alginate/ chitosan millicapsules and to assess survival rates during storage and the viability of the encapsulated probiotics under simulated GI conditions.

2. Materials and method

2.1. Materials, bacterial strains, and media

Sunflower oil with a density of 918.8 kg/m^3 was provided by Nina Co, Iran, to make an emulsion with sterilized deionized water. Calcium chloride ($CaCl_2.2\ H_2O$, 147.01 g/mol), sodium alginate (1.37 M/G ratio, 1.57× 10^5 g/mol, low viscosity), and low molecular chitosan powders were purchased (Sigma Aldrich, USA), and used as supplied. Surfactants (Tween 20 with a hydrophilic–lipophilic balance (HLB) = 16.7 and PGPR 90 with HLB= 1.5) and glacial

acetic acid were also used as supplied (Merch, Germany). *Lactobacillus plantarum* PTCC 1896™ (A7), was obtained from the microbial culture collection of IROST (Iranian Research Organization for Science and Technology, Tehran, Iran), and *Bifidobacterium animalis* subsp. *Lactis* (BB-12®) was purchased from Chr. Hansen (Hørsholm, Denmark). Both microorganisms were isolated as probiotic bacteria from the stool of breastfed babies. De Man, Rogosa and Sharpe (MRS) agar and broth, L-Cysteine hydrochloride, Anaerocult® A gas pack, hydrochloric acid, sodium hydroxide, potassium dihydrogen phosphate, and pepsin were obtained from Merck (Darmstadt, Germany). Tri-sodium citrate, bile salts, and pancreatin were supplied by Sigma-Aldrich (St. Louis, Missouri, USA).

2.2. Methods

2.2.1. Activation of Probiotics

To activate the lyophilized *Lactobacillus*, the A7 strain was propagated in MRS Broth medium and incubated at 37 °C for 18 h. BB-12® is an obligate anaerobic bacterium. Therefore, to create favorable conditions for lyophilized *Bifidobacterium*, 0.5 g/L L-Cysteine hydrochloride (Cys-HCl) was added to the MRS broth, and placed in an anaerobic jar with an Anaerocult® A gas pack at 37 °C for 24-48 h (Zaeim, Sarabi-Jamab, Ghorani, & Kadkhodaee, 2019).

2.2.2. Water/Oil (W/O) emulsion preparation

Preparation of W/O emulsion as the dispersed phase of millifluidic device was performed according to a modification of the method of Martins, et al. (2017). 80 ml of sunflower oil was mixed with 0.8 g PGPR 90 using a high shear mixer (Ultra-Turrax T25,

Germany) at 18000 rpm for 1 min. 20 ml of sterilized deionized water was then added drop wise and mixed at 18000 rpm for 2 min. About 10^{10} CFU g^{-1} activated probiotic cells were harvested by centrifugation (Hermle Z-32 HK, Germany) at 3500×g and 4 °C for 10 min and the pellets were immediately washed thoroughly with sterilized distilled water to eliminate any residual MRS broth. Finally, 1 g of probiotic cells were dissolved in 1 ml sterilized deionized water, dispersed separately to 99 ml of emulsion, and mixed gently using a magnetic stirrer (IKA-RCT basic, Germany) at room temperature for 30 min to make homogeneous feed solutions. 1 ml samples were taken to count viable probiotics in the initial solution. It should be noted that the addition of bacterial pellets to the W/O emulsion was performed in sterile conditions.

2.2.3. Preparing alginate, chitosan and calcium chloride solutions

The calcium chloride solution used as the gelling bath was prepared by dissolving 30 g of powder in 1 liter of sterilized deionized water. Different concentrations of sodium alginate (20, 25, 30 g/L) were also made up using sterilized distilled water. After 24 h hydration, 6 g/L Tween 20 was added to the alginate solutions to reduce surface tension when forming the alginate droplet. Chitosan powder (15 g/L) was mixed with sterilized water containing 0.1 M acetic acid. After adjusting the pH to 5.5, the coating solution was continuously agitated for 1 hour using a magnetic stirrer.

2.2.4. Characterization of emulsion, and alginate solutions

2.2.4.1. Emulsion stability

The stability of the W/O emulsion was assessed by centrifugation and calculating the weight of the supernatant. Freshly formed emulsion (M_0) was centrifuged at 5000 rpm for 10 min (Sciarini, Maldonado, Ribotta, Pérez, & León, 2009). After separating the supernatant part (M_1),

stability of the emulsion was determined as a ratio of supernatant to the initial weight of the emulsion (**Eq. 1**).

$$ES\ (\%) = (M_1/M_0) \times 100 \quad \textbf{(1)}$$

2.2.4.2. Flow behavior of emulsion and alginate solutions

Viscosity of emulsion and alginate solutions at shear rates of 1-295 (s^{-1}) were determined at 25℃ using a rotary viscometer (RVDV-II, Brookfield, USA) with an SC-18 spindle. The flow curves were fitted to the Power-law model according to **Eq. (2)**, where σ is the shear rate, n is the flow behavior index, K is the consistency coefficient, and $\gamma^{\cdot}$ Is the shear rate.

$$\sigma = K.\gamma^n \quad \textbf{(2)}$$

Simulated shear rates of samples in the glass tube were calculated as follows (**Eq. 3**) (Wohl, 1968), and the viscosities were determined at these shear rates.

$$\gamma = (3 + \frac{1}{n})\ Q/\pi r^3 \quad \textbf{(3)}$$

where Q, r, n, and γ are the flow rate of the continuous phase (m^3/s), the inner radius of tube (m), flow behavior index, and simulated shear rate (s^{-1}), respectively.

2.2.5. Millifluidic encapsulation of W/O emulsion

A millifluidic device with coaxial geometry was made (Farahmand, et al., 2021; Martins, et al., 2017). The W/O emulsion as the dispersed phase was pumped (New Era, NE-300, USA) using a Teflon tube (interior and outside diameters: ID=0.6 and OD= 1.5 mm) at flow rates of 0.5- 0.7 ml/min. A larger Teflon tube (ID= 0.9 and OD= 2 mm) was used to pump an alginate-Tween solution as continuous phase at flow rates of 0.8- 1.2 ml/min. The droplets were

generated by co-flowing the two phases in a glass tube (ID= 3.2, OD= 5 mm, length: 20 cm) to exert shear forces between phases. The pinched-off droplets were collected under sterilized conditions in the gelling bath ($CaCl_2$ 30 g/L) and stirred at 50 rpm for 30 min, then suspended in 15 g/L chitosan solution for 15 min. After rinsing with sterilized water, the coated millicapsules were stored in sterilized bottles suspended in 15 g/L $CaCl_2$ solution at 4 °C.

2.2.6. Characterization of the millicapsules

2.2.6.1. Dimensions and sphericity

The sizes of at least 20 millicapsules were measured using Image J software (USA) and sphericity factors (SF) were calculated from this data. A digital microscope (Dino-lite pro, Taiwan) was used to capture all experimental runs (1280×1024 resolution and ×30 magnification), the SF values were calculated as below (Davarcı, Turan, Ozcelik, & Poncelet, 2017) (**Eq. 4**):

$$SF= (2\ d_{min})/ (d_{max}+ d_{min}) \quad (\mathbf{4})$$

Where d denotes the millicapsule diameter. The SF values above 0.95 confirm a spherical shape, and 0.9 <SF< 0.95 implied the oval and pear shape.

2.2.6.2. Efficiency of emulsion encapsulation (EE)

The amount of non-encapsulated emulsion was determined by collecting the millicapsules from the gelling bath and rinsing them three times with sterilized distilled water on a sieve covered with a filter paper (Whatman 41). After drying the filter paper in an oven (Binder-FP53,Germany) (105℃) to constant weight, the EE was calculated as the difference

between the initial weight of the emulsion (W_i), and that of the non-encapsulated emulsion (W_{ne}) (**Eq. 5**) (Chan, 2011):

$$EE\ (\%) = (W_i - W_{ne}) / W_i \times 100 \quad \textbf{(5)}$$

2.2.7. The survival efficiency of encapsulated probiotics

The encapsulation efficiency of the probiotics was validated based on the number of viable cells before and after the millifluidic encapsulation process using a plate count method, and the percentage of surviving bacteria was calculated as follows:

$$EY = \left(\frac{\log_{10} N}{\log_{10} N0}\right) * 100 \quad \textbf{(6)}$$

where N and N_0 are the number of cells in the millicapsules and in the initial feed solution (CFU g/1) (Haghshenas, et al., 2015; Heidebach, Först, & Kulozik, 2010).

To count the live cells before encapsulation, the feed solution containing viable cells was serially diluted in Ringer's solution (pH 7.0), plated, incubated, and counted. After encapsulation, the millicapsules were decomposed in 50 mM sodium citrate solution. Then the quantity of released live cells were estimated as described above.

2.2.8. Bacterial survival under simulated gastrointestinal conditions

To make the simulated gastric fluid, 3.2 g/L pepsin in 2 g/L NaCl solution was dissolved and the pH of the solution was adjusted to 2.5 by using 1 and 5 M HCl. Simulated intestinal fluid was prepared by dissolving 1 g/L pancreatin and 20 g/L bile salts in 0.1 mol/L potassium

dihydrogen phosphate solution, and finally, pH of the solution was adjusted to pH7.4 by 0.1 and 1 M NaOH. Both the simulated gastric and intestinal solutions were then sterilized by a 0.2 μm cellulose acetate syringe filter and pre-warmed to 37 °C using a shaker water bath. 1 g of millicapsule solution was added to glasses containing 9 ml of simulated gastric fluid and agitated gently in a shaker incubator at 37 °C for 2 h. Following this step, using sterilized Whatman No. 4 filter paper, the millicapsules were separated from the simulated gastric solution and introduced into 9 ml of simulated intestinal fluid and stirred for at least 2 h under similar conditions (Annan, Borza, & Hansen, 2008; Cook, Tzortzis, Charalampopoulos, & Khutoryanskiy, 2011; Rao, Shiwnarain, & Maharaj, 1989). Sampling was performed every hour, and the number of live bacteria was determined by the plate count method. First, the millicapsules were entirely disintegrated in 50 mM sodium citrate solution for 15 to 30 min at room temperature on a shaker. After the bacteria were released from the millicapsule structure, a 1 ml sample was taken, serially diluted using sterile ringer solution, and then spread on MRS agar plates. Under at 37 °C incubation conditions the colonies appeared after 48-72 h. Bacterial count experiments were made in triplicate, and the data were presented as mean± standard deviation (Cook, et al., 2011; Heidebach, et al., 2010; Solanki, et al., 2013).

2.2.9. Viability of bacteria during storage time

The millicapsules containing live probiotics were maintained at -18 °C for 6 months. The count of viable cells was determined monthly by the method described in the previous section.

2.2.10. Statistical analysis

The processing parameters, including alginate concentration (X_1, [Alg]: 20-30 g/l), the flow rate of alginate (X_2, Q_{Alg}: 0.8-1.2 ml/min), and the flow rate of emulsion (X_3, $Q_{emulsion}$: 0.5-0.7 ml/min), were optimized by response surface methodology (RSM) with central composite design (CCD). In 20 experimental runs with 6 central points (**Table.** 1), characteristics of the millicapsules on the EE (Y1), size (Y2), and sphericity (Y3) were assessed. The data of dependent variables were fitted to a second-order polynomial equation (**Eq. 6**):

$$Y = \beta_0 + \sum_{i=1}^{n} \beta_i X_i + \sum_{i=1}^{n-1} \sum_{j=i+1}^{n} \beta_{ij} X_i X_j + \sum_{i=1}^{n} \beta_{ii} Xi^2 \quad \textbf{(6)}$$

Where Y is the dependent variable, X_i and X_j are independent variables, and β_0, β_i, β_{ii}, β_{ij} are regression coefficients. Optimization was analyzed by Design expert software (version 10, stat-Ease, USA) based on maximizing the EE, SF, and size.

Insert Table. 1 about here

Data analysis for bacterial survival under simulated gastrointestinal conditions and during storage at -18 °C, was carried out using the IBM® SPSS® software platform (version 20.0). One-way analysis of variance (ANOVA) was used to determine if there were significant ($p<0.05$) differences between sample means. Mean comparisons were performed using Duncan's Test. All the experiments were performed in triplicate, and the data were averaged and reported as mean± standard deviation.

3. Results and discussion

3.1. Characterization of the continuous and dispersed phases

3.1.1. Stability of the water/oil (W/O) emulsion

Monodispersed droplets have an effect on the stability of W/O emulsions, their controlled release, and physical characteristics such as viscosity, particle size, microstructure, and shape. In addition to processing parameters, emulsion compositions also have a significant impact on the long-term stability of W/O emulsions (Nisisako & Torii, 2008; J. Xu, Li, Tan, Wang, & Luo, 2006). In this research, W/O emulsion containing probiotics was selected as the dispersed phase of the millifluidic device, which must remain stable to protect the bacteria. Emulsion stability was assessed at 25 °C (room temperature) as a function of storage time (**Fig. 1**) and centrifugal stability. As can be seen in **Fig.1**, it can be visually observed that our W/O emulsion as a carrier of probiotics was stable up to 36 h. Minimal phase separation and coalescence were observed during the storage time. According to our results, the centrifugal stability of W/O emulsion was 81.42%. This is because polyglycerol polyricinoleate (PGPR) could migrate quickly to the water/oil interface and form a structured interface that boosts steric hindrance thus playing a role in emulsion stability (Okuro, Gomes, Costa, Adame, & Cunha, 2019). Therefore, reducing the interfacial tension between the two phases by using PGPR could simplify the fabrication of dispersed phase droplets at the junction of two fluids in the tube. These droplets are formed in tube through exerting the shear stress of the continuous phase on the dispersed phase (Costa, Gomes, Ushikubo, & Cunha, 2017).

Insert figure.1 about here

3.1.2. Flow behavior of phases

The flow behavior parameters of the continuous and dispersed phases at various concentrations and flow rates of the millifluidic device are reported in **Table .2**. The curve of viscosity versus shear rates of phases (data not shown) depicted shear-thinning (pseudoplastic) behavior of alginate solutions at three different concentrations. This behavior is also confirmed by Power-law model fitting (**Table. 2**) with a flow behavior index of less than 1 ($n<0.72$). The viscosity distribution of non-Newtonian fluids around a droplet in the tube depends on the shear rate, which could change the droplet size (Vagner, Patlazhan, & Serra, 2018). Hence, after calculating of the simulated shear rate in the tube according to **Eq. 3**, viscosity in the tube was also reported in **Table. 2**. It should be noted that as the alginate concentration was increased from 20 to 30 g/l, the viscosity also increased due to individual alginate molecules overlapping and forming intermolecular junctions (Funami, et al., 2009). The consistency coefficient (k) in continuous phase solutions also increased with increasing concentration (from 317.6± 0.9 to 1853.08± 1.07 mP.s). Shear-thinning behavior is associated with cluster breakup and chain alignment, leading to viscosity reduction of solution during movement, so increasing the flow rate of solution favors the flow process (Costa, et al., 2017). The W/O emulsion showed a more pronounced Newtonian behavior (higher n value). The consistency index (k) and viscosity were also lower as compared with alginate solutions. Sunflower oil + PGPR showed Newtonian rheological behavior, that could be attributed to the long chain of triacylglycerols structure and chain unsaturation (Gomes, Costa, & Cunha, 2018; Meirelles, et al., 2021).

The viscosities of both phases are important from two aspects: first, viscosity shows an impact on the droplet size. For example, Guillot and Colin (2005) and Garstecki, Stone, and Whitesides (2005) reported a reverse effect of continuous phase viscosity on the droplet size.

Furthermore, increasing the dispersed phase viscosity will change both the squeezing pressure and the viscous shear which affect droplet detachment. More viscous liquid is pushed out of the tube before the collapse of the droplet neck. Slow breakup of the dispersed fluid results in large droplet formation. In other words, a larger shear force is needed to overcome the interfacial tension of the high viscosity dispersed phase (Zheyu Liu, Chai, Chen, Hejazi, & Li, 2021). Second, the continuous phase viscosity above 500 mPa.s, will cause problems both with pumping and the final shape of the millicapsules (Moghadam, Samimi, Samimi, & Khorram, 2008). As shown in **Table. 2**, both phases at all simulated shear rates had viscosity values lower than the mentioned critical value. Also, viscosity value of the dispersed phase was lower than the continuous phase ($Q_{Alg} > Q_{emulsion}$).

Insert Table. 2 about here

3.2. Characterization of the millicapsules

To study the effect of process variables (flow rates of two phases, and alginate concentration) on the millicapsule properties (encapsulation efficiency, size, and sphericity), ANOVA was used and confirmed the validity of the experimental design responses (see **Supplementary, Table. 1**). The fitted equations for each response were written in **Table. 3**.

Insert Table. 3 about here

3.2.1. Effect of independent variables on EE

High encapsulation efficiency (EE) is the main advantage in production of larger capsules (Chen, Li, Liu, & Meng, 2017). The larger capsules enable greater protection to the core, due to the reduced rate of core penetration of oxygen (Silva, et al., 2018), and by providing an effective barrier against harsh conditions. Significant interactions among the variables affecting EE are shown in **Fig. 2, A-C**. As shown in **Fig. 2 (A)**, the addition of the alginate flow rates (0.8 to 1.2 ml/min) could improve the EE of W/O emulsion from 37.5± 0.2 to 62.15± 0.56%.

The distance between detached droplets from the millifluidic tube and droplet size can be controlled by tuning flow rates. The effect of forces exerted on the droplets in the millifluidic tube (Farahmand, et al., 2021), relate to increasing the flow rate of the continuous phase leading to higher pressure on the interface, higher velocity gradient, and consequently higher viscous forces, which may break the dispersed phase (W/O emulsion) into droplets inside the millifluidic tube. The time required for the detachment of droplets from the tube will be shortened. Subsequently, a lower volume fraction of fluid in the droplet leads to a reduction in size and to complete covering by the continuous phase (Cramer, Fischer, & Windhab, 2004; Fu, Wu, Ma, & Li, 2012). The differences between the viscosity and flow rates of both phases led to an increase in intromission of the alginate phase (shell) into the detached droplets compared to the case when a W/O emulsion dispersed phase forms the core. This higher shell/core ratio caused a thicker shell in the millicapsule due to more interactions of alginate and calcium ions, hence becoming more effective in entrapping the emulsion core (higher EE).

Regarding the EE (**Fig. 2, B**), it was possible to establish an inverse relationship between flow rate of the W/O emulsion and EE. More resistance to the continuous phase induced at higher flow rates of the dispersed phase led to larger droplets. Benavides, Cortés, Parada, and

Franco (2016) also observed this trend in capsules of thyme essential oil produced by ionic-gelation, noting that entering a higher amount of oil as dispersed phase led to the presence of a significant amount near the capsule surface due to limitation of capsule capacity. This thin shelled overloaded capsule could not maintain a core in the gelling bath, so the EE was decreased. A significant interaction between flow rates of the continuous phase and the dispersed phase is shown in **Fig. 2 (C)**.

As demonstrated in **Fig. 2 (A, B)**, augmenting the alginate concentration (and hence viscosity) from 20 to 30 g/l led to higher EE values (from 61.53± 0.74 to 98.9± 0.25 %). Greater availability of active sites in the alginate chains could bind to Ca^{2+} and with higher degree of cross-linking. Rousseau, Le Cerf, Picton, Argillier, and Muller (2004) show similar results showing that the alginate concentration has a considerable effect on the mesh size of capsules, with larger pore sizes created at lower concentrations of alginate. Hence, the movement of lipid droplets to the surface of porous capsules and also the surrounding aqueous medium is facilitated. This high leakage in the gelling step plays a role in the EE reduction: a higher concentration of the continuous phase induces higher detaching forces, which are exerted on the droplet at the tip of the tube (Martins, et al., 2017).

Insert figure.2 about here

3.2.2. Effect of independent variables on size

Droplet size and the millicapsule size directly determine the quality of the encapsulated compounds, the characteristics of produced emulsion, and the amount of oil recovery (C. Xu & Xie, 2017). The diameter of millicapsules varied from 4.37± 0.1 to 4.68± 0.02 mm at different experimental runs (**Fig. 2, D-F**). Cavalheiro, et al. (2019) also produced probiotic capsules with a millimeter scale. According to Chen, et al. (2017), macrocapsules contain a higher load of probiotics, increasing the EE.

The interaction of the flow rate and concentration (**Fig. 2, D**) showed that millicapsule size decreased in inverse proportion to the alginate flow rate (Q_{Alg}) as it varied from 0.8 to 1.2 ml/min. Droplets decrease in size when the velocity of the continuous phase increases because of the larger shear stress exerted on the interface (Lan, Jing, Guo, & Li, 2017). Cramer, et al. (2004) investigated the effect of flow rates, fluid viscosity, and interfacial tension on droplet size. Their results indicate that increasing the flow rate of the continuous phase means more efficient detachment from the tube, and consequently, a reduction in droplet size. Furthermore, the effect of shear stress on the continuous phase at higher flow rates could be more significant than interfacial tension between the dispersed phases (Meirelles, et al., 2021).

Significant interactions between the flow rate of the dispersed phase and concentration of the continuous phase (**Fig. 2, E**) are demonstrated by the steep slope of the plot of emulsion flow rate ($Q_{emulsion}$), indicating the sensitivity of size to this parameter. It was found that the largest millicapsule (4.68± 0.13 mm) was obtained at $Q_{emulsion}$ of 0.7 ml/min, due to the high loading of the emulsion into droplets compared to the alginate solution. Zheyu Liu, et al. (2021) and Amine, et al. (2020) examining millifluidic methods, also reported that an increase in flow rate of the dispersed phase led to increasing the droplet size, which they related to the

magnitude of shear and inertial forces. A similar trend is also shown in the three-dimensional interaction plot of the phases flow rates (**Fig. 2, F**).

It was found from **Fig. 2, D** that alginate concentration ([Alg]) had an adverse effect on the millicapsule diameter. Based on **Table. 2**, the higher concentration of continuous phase (with high viscosity in millifluidic tube) exerted a higher drag force on the dispersed phase and also quickly broke up the small droplets. This finding was in accordance with other millifluidic studies (Farahmand, et al., 2021; Martins, et al., 2017).

3.2.3. Effect of independent variables on SF

The minimal surface/volume ratio of spherical shapes results in a lower release rate of any loaded compounds. **Fig. 2 (G-I)** illustrates the three-dimensional response surface plots as a function of the continuous phase concentration and flow rates of both phases. As can be seen, there were significant interactions among the independent variables for response to sphericity factor (SF). SF values were in the range of 0.85-0.98, which indicated millifluidic method conditions that produce completely round capsules. As depicted in **Fig. 2 (G)**, the highest sphericity of millicapsules was obtained at an alginate flow rate of 1.2 ml/min. Furthermore, the favorable effect of alginate flow rate is amplified at higher alginate concentrations (SF=99.3). Increasing the alginate flow rate results in the high drag force. Consequently, detaching time of droplet is shortened, and lower fluid accumulation produces smaller droplets (Lee, Ravindra, & Chan, 2013). According to the momentum equation (Momentum=mass× velocity), when two droplets fall from the same height, the smaller one has less momentum (ie impulse at collision). Therefore, smaller droplets are obtained at higher alginate flow rates.

Fig. 2 (H, I) shows that the W/O emulsion flow rate had an inverse effect on sphericity. By immersing the droplet in the gelling bath, viscous forces within the droplet retain the spherical shape while drag forces induced via the bath tend to disrupt the capsule. As the flow rate of the dispersed phase was increased, larger droplets with thinner shells were obtained. These droplets either could not tolerate the forces experienced inside the gelling bath, or were disintegrated on the surface due to high momentum.

In **Fig. 2 (H)**, we can see that more spherical millicapsules were formed at higher concentrations of alginate. There is a direct relationship between penetration depth into the gelling bath and sphericity of capsules. Higher droplet viscosity of allows a more spherical shape to form as a result of deeper penetration (Davarcı, et al., 2017). Moreover, a strong network-like structure is made from an increase in cross-linking reactions within the high viscous droplets, improving the shape of the millicapsule.

3.2.4. Optimization of the millifluidic process and model validation

Optimized amounts of [Alg]= 30g/l, Q_{Alg}= 1.2 ml/min, and $Q_{emulsion}$= 0.5 ml/min to achieve the maximum EE (99.34%), size (4.42 mm), and SF (0.98) were obtained using the numerical point prediction method. The target accuracy criterion was 0.92. The reliability of predicted optimized conditions was tested with a series of experiments using the optimized variables, and the results were measured as 98.17± 0.5%, 4.49± 0.19 mm, and 0.97± 0.01. These results agreed with the corresponding predicted values and confirmed the high accuracy of the models in predicting the millifluidic process. **Fig. 3** depicts the calcium-alginate millicapsules with W/O emulsion core covered with a chitosan shell, corroborating the proper application of the millifluidic method to achieve emulsion-filled delivery system. The analysis of millicapsule

revealed spherical shape with uniform size, smooth surface, and emulsion distributed throughout the matrix.

Insert figure.3 about here

3.3.Evaluation of encapsulated probiotic efficiency at the optimized conditions

During encapsulation, probiotic cells are often exposed to the environmental challenges, such as oxygen, thermal, mechanical stresses or severe acidic conditions in the stomach that may affect cell viability and proliferation. Therefore, depending on the encapsulation method and the amount of stress applied during it, the encapsulation efficiency of probiotics will vary (Okuro, Thomazini, Balieiro, Liberal, & Fávaro-Trindade, 2013; Sathyabama & Vijayabharathi, 2014).

The cell live number of *Lactobacillus plantarum* and *Bifidobacterium animalis* in the initial feed solution was 10.08± 0.07 and 10.56± 0.04 CFU g^{-1}, respectively. After millifluidic process, the number of viable cells was dropped to 9.31± 0.05 Log CFU g^{-1} for *Lactobacillus plantarum* and 9.59± 0.06 Log CFU g^{-1} for *Bifidobacterium animalis*. Tests indicate that less than 1 log cycle of *Lactobacillus plantarum and* about 1 log cycle of *Bifidobacterium animalis* were either inactivated or lost into the collector solution during the millifluidic encapsulation method. However, the survival efficiency of A7 and BB-12® was found to be close to 92.36% and 90.81%. The encapsulation efficiency of probiotics is generally in the range of 60-95% and an EE value greater than 90% has rarely been reported (Pitigraisorn, et al., 2017; Silva, et al., 2016), so the encapsulation technique and operational conditions play a key role in achieving

high encapsulation efficiency (Y. Liu, Sun, Sun, & Wang, 2016; Pitigraisorn, et al., 2017; Shi, et al., 2013).

3.4. Effect of the millifluidic encapsulation on viability of probiotics under the simulated GI conditions

After the exposure of encapsulated *Lactobacillus plantarum* (A7) and *Bifidobacterium animalis* subsp. *lactis* (BB-12®) to simulated gastric fluid, the number of live bacteria in both samples decreased by about one logarithmic cycle (**Table. 4**). The results also showed that after 2 h of exposure of the encapsulated A7 to simulated gastric conditions, less than one other logarithmic cycle in the number of live bacteria was observed, while for BB-12®, more than one logarithmic cycle decreased. This effect can be attributed to the diffusion of small hydrogen ions (H+) from the simulated gastric fluids into the microgels that deactivate the probiotic cells (Zhang, et al., 2021).

By transferring the samples to simulated intestinal fluid and incubating for 2 h, it was observed that the live cell number in both samples did not decrease; In other words, the millifluidic encapsulated microorganisms tolerated the harsh conditions of the simulated intestinal environment (particularly the presence of bile salts and the pancreatin), and their viability remained almost constant. In some cases, an increase in the growth rate of bacteria was observed, which can be attributed to the adaptation of the microorganism to the simulated conditions of the intestine, as well as the use of bile salts as a nutrient source.

Finally, the results showed that when *Lactobacillus plantarum* was exposed to simulated GI conditions for 4 h, approximately 7.50 log CFU mL^{-1} of bacteria survived. For *Bifidobacterium animalis* subsp. *Lactis*, at the end of the time of exposure to simulated conditions of the GI tract, the number of live cells was about 7.54 log CFU mL^{-1}. This section

showed that the encapsulation of probiotic bacteria in the alginate-chitosan millicapsule improves the viability of cells as it passes through the GI tract. These results are also in the line with previous publications on the development of core-shell microencapsulation systems (Laelorspoen, et al., 2014; Silva, et al., 2016; Zhang, et al., 2021) as well as W/O microfluidic emulsions for encapsulation of probiotics (Quintana, et al., 2021).

Insert Table. 4 about here

3.5. Effect of the millifluidic encapsulation on the viability of probiotics during storage

One of the most critical factors in encapsulating of bioactive compounds such as probiotic bacteria is their stability during storage. Therefore, role of the millifluidic encapsulation method as well as biopolymers forming the capsule wall in maintaining the survival of probiotic bacteria during shelf-life was investigated. It should be noted that the loading of probiotics within the millicapsule has a direct effect on their survival rate during passage through the simulated GI tract and storage time. In this study, the initial number of both *Lactobacillus plantarum* and *Bifidobacterium animalis* subsp. *Lactis* live cells before encapsulation were about 10 log CFU mL^{-1}.

Table. 5 shows the number of surviving encapsulated probiotics when stored at -18 °C for six months. As can be seen, the survival of both bacteria decreased by about 4 logarithmic cycles. Concerning to *Lactobacillus plantarum*, the number of viable cells after production was about 9 log cycles, indicating a reduction of about 1 log cycle during the millifluidic

encapsulation process. By the end of the first month of storage, there was only a decrease of one log cycle compared to the initial number of microorganisms; However, viable counts remained almost unchanged in the millicapsule after the second month. Meanwhile, during the third and fourth months, the viable cells were reduced from 8.07± 0.23 to about 7 log CFU g^{-1}, and in the fifth and sixth months, the number of living bacteria reached 6.39± 0.07 and 5.41± 0.08 Log CFU g^{-1}, respectively. In other words, the survival rate of millifluidic encapsulated *Lactobacillus plantarum* is acceptable only until the end of the fifth month, which is considered acceptable according to the standards defined for probiotic products that have been recommended that food products should contain 6 Log CFU g^{-1} or more viable probiotics to exhibit their beneficial health effects (Zhang, et al., 2021).

Regarding the survival of *Bifidobacterium animalis* subsp. *Lactis* during six-month shelf-life tests (**Table. 5**), on the first day of counting (initial number after production), the number of millifluidic encapsulated bacteria was more than 9 logarithmic cycles. After one month of storage, the live cells were reduced by about one logarithmic cycle: the number of surviving *Lactobacillus plantarum* was 8.36± 0.14 Log CFU g^{-1}. The number of live cells of BB-12® remained about 7 log cycles until the end of the fourth month of storage and reached about 6, and 5 log cycles in the fifth, and sixth months.

The results of the survival study during the storage time of two probiotics (A7 and BB-12®) encapsulated by millifluidic method showed a significant decrease over time ($p<0.05$). However, after 5 months of storage, their number of live cells per gram of capsule was still in accordance with the standard definition of probiotics. A similar pattern of reduction in the viability of probiotics during the storage was also reported by Silva, et al. (2016) for *L. paracasei* BGP-1 incorporated sunflower oil or coconut fat matrix and co-extruded with

alginate-shellac blend, Silva, et al. (2018) for *L. acidophilus LA3* co-extruded by the blend of alginate-shellac, and Zhang, et al. (2021) for *Bifidobacterium pseudocatenulatum G7* co-encapsulated within calcium alginate microgels, colloidal antacid and nano-emulsion lipid droplets.

Insert Table. 5 about here

3.6. Conclusion

Millifluidic/direct gelation method was applied as a platform to produce the W/O emulsion-filled millicapsule for encapsulation of two probiotic bacteria: *Bifidobacterium animalis* subsp. *lactis* and *Lactobacillus plantarum*. The effect of process variables on morphology, size, and encapsulation efficiency of millicapsule was studied. Optimal emulsion-filled millicapsules had uniform spherical shapes of monodispersed size. A high efficiency of bacterial survival was achieved after the encapsulation process (reduction about one log cycle). The millicapsules also strongly protected both strains against the simulated GI conditions. The numbers of live cells were still in accordance with the standard definition of probiotics after six months of storage. Accordingly, the utility of the millifluidic encapsulation method paves the way for fabrication of a unique carrier for probiotic bacteria. Furthermore, encapsulation of lipophilic compounds in the oil part and hydrophilic compounds in the water part of emulsion loaded in millicapsules can be exploited co-encapsulation in various domains, an advance which needs further investigation.

References

Alehosseini, A., Sarabi-Jamab, M., Ghorani, B., & Kadkhodaee, R. (2019). Electro-encapsulation of Lactobacillus casei in high-resistant capsules of whey protein containing transglutaminase enzyme. *LWT, 102*, 150-158.

Amine, C., Boire, A., Davy, J., Reguerre, A.-L., Papineau, P., & Renard, D. (2020). Optimization of a Droplet-Based Millifluidic Device to Investigate the Phase Behavior of Biopolymers, Including Viscous Conditions. *Food Biophysics, 15*(4), 463-472.

Annan, N., Borza, A., & Hansen, L. T. (2008). Encapsulation in alginate-coated gelatin microspheres improves survival of the probiotic Bifidobacterium adolescentis 15703T during exposure to simulated gastro-intestinal conditions. *Food Research International, 41*(2), 184-193.

Anselmo, A. C., McHugh, K. J., Webster, J., Langer, R., & Jaklenec, A. (2016). Layer- by- layer encapsulation of probiotics for delivery to the microbiome. *Advanced Materials, 28*(43), 9486-9490.

Benavides, S., Cortés, P., Parada, J., & Franco, W. (2016). Development of alginate microspheres containing thyme essential oil using ionic gelation. *Food Chemistry, 204*, 77-83.

Cavalheiro, C. P., Ruiz- Capillas, C., Herrero, A. M., Jiménez- Colmenero, F., Pintado, T., de Menezes, C. R., & Fries, L. L. M. (2019). Effect of different strategies of Lactobacillus plantarum incorporation in chorizo sausages. *Journal of the Science of Food and Agriculture, 99*(15), 6706-6712.

Chan, E.-S. (2011). Preparation of Ca-alginate beads containing high oil content: Influence of process variables on encapsulation efficiency and bead properties. *Carbohydrate Polymers, 84*(4), 1267-1275.

Chen, H.-Y., Li, X.-Y., Liu, B.-J., & Meng, X.-H. (2017). Microencapsulation of Lactobacillus bulgaricus and survival assays under simulated gastrointestinal conditions. *Journal of Functional Foods, 29*, 248-255.

Cook, M. T., Tzortzis, G., Charalampopoulos, D., & Khutoryanskiy, V. V. (2011). Production and evaluation of dry alginate-chitosan microcapsules as an enteric delivery vehicle for probiotic bacteria. *Biomacromolecules, 12*(7), 2834-2840.

Costa, A. L. R., Gomes, A., Ushikubo, F. Y., & Cunha, R. L. (2017). Gellan microgels produced in planar microfluidic devices. *Journal of Food Engineering, 209*, 18-25.

Cramer, C., Fischer, P., & Windhab, E. J. (2004). Drop formation in a co-flowing ambient fluid. *Chemical Engineering Science, 59*(15), 3045-3058.

Davarcı, F., Turan, D., Ozcelik, B., & Poncelet, D. (2017). The influence of solution viscosities and surface tension on calcium-alginate microbead formation using dripping technique. *Food Hydrocolloids, 62*, 119-127.

Farahmand, A., Emadzadeh, B., Ghorani, B., & Poncelet, D. (2021). A comprehensive parametric study for understanding the combined millifluidic and dripping encapsulation process and characterisation of oil-loaded capsules. *Journal of Microencapsulation*(just-accepted), 1-42.

Fu, T., Wu, Y., Ma, Y., & Li, H. Z. (2012). Droplet formation and breakup dynamics in microfluidic flow-focusing devices: From dripping to jetting. *Chemical Engineering Science, 84*, 207-217.

Funami, T., Fang, Y., Noda, S., Ishihara, S., Nakauma, M., Draget, K. I., Nishinari, K., & Phillips, G. O. (2009). Rheological properties of sodium alginate in an aqueous system during gelation in relation to supermolecular structures and Ca^{2+} binding. *Food Hydrocolloids, 23*(7), 1746-1755.

Garstecki, P., Stone, H. A., & Whitesides, G. M. (2005). Mechanism for flow-rate controlled breakup in confined geometries: A route to monodisperse emulsions. *Physical Review Letters, 94*(16), 164501.

Gomes, A., Costa, A. L. R., & Cunha, R. L. (2018). Impact of oil type and WPI/Tween 80 ratio at the oil-water interface: Adsorption, interfacial rheology and emulsion features. *Colloids and Surfaces B: Biointerfaces, 164*, 272-280.

Guillot, P., & Colin, A. (2005). Stability of parallel flows in a microchannel after a T junction. *Physical Review E, 72*(6), 066301.

Haghshenas, B., Nami, Y., Haghshenas, M., Abdullah, N., Rosli, R., Radiah, D., & Yari Khosroushahi, A. (2015). Bioactivity characterization of Lactobacillus strains isolated from dairy products. *Microbiologyopen, 4*(5), 803-813.

Heidebach, T., Först, P., & Kulozik, U. (2010). Influence of casein-based microencapsulation on freeze-drying and storage of probiotic cells. *Journal of Food Engineering, 98*(3), 309-316.

Holkem, A. T., Raddatz, G. C., Nunes, G. L., Cichoski, A. J., Jacob-Lopes, E., Grosso, C. R. F., & de Menezes, C. R. (2016). Development and characterization of alginate microcapsules containing Bifidobacterium BB-12 produced by emulsification/internal gelation followed by freeze drying. *LWT-Food Science and Technology, 71*, 302-308.

Khaneghah, A. M., Abhari, K., Eş, I., Soares, M. B., Oliveira, R. B., Hosseini, H., Rezaei, M., Balthazar, C. F., Silva, R., & Cruz, A. G. (2020). Interactions between probiotics and pathogenic microorganisms in hosts and foods: A review. *Trends in Food Science & Technology, 95*, 205-218.

Laelorspoen, N., Wongsasulak, S., Yoovidhya, T., & Devahastin, S. (2014). Microencapsulation of Lactobacillus acidophilus in zein–alginate core–shell microcapsules via electrospraying. *Journal of Functional Foods, 7*, 342-349.

Lan, W., Jing, S., Guo, X., & Li, S. (2017). Study on "interface–shrinkage–driven" breakup of droplets in co-flowing microfluidic devices. *Chemical Engineering Science, 158*, 58-63.

Lee, B. B., Ravindra, P., & Chan, E. S. (2013). Size and shape of calcium alginate beads produced by extrusion dripping. *Chemical Engineering & Technology, 36*(10), 1627-1642.

Li, C., Bei, T., Niu, Z., Guo, X., Wang, M., Lu, H., Gu, X., & Tian, H. (2019). Adhesion and colonization of the probiotic Lactobacillus rhamnosus labeled by dsred2 in mouse gut. *Current Microbiology, 76* (7), 896-903.

Liu, Y., Sun, Y., Sun, L., & Wang, Y. (2016). In vitro and in vivo study of sodium polyacrylate grafted alginate as microcapsule matrix for live probiotic delivery. *Journal of Functional Foods, 24*, 429-437.

Liu, Z., Chai, M., Chen, X., Hejazi, S. H., & Li, Y. (2021). Emulsification in a microfluidic flow-focusing device: Effect of the dispersed phase viscosity. *Fuel, 283*, 119229.

Liu, Z., Liu, F., Wang, W., Sun, C., Gao, D., Ma, J., Hussain, M. A., Xu, C., Jiang, Z., & Hou, J. (2020). Study of the alleviation effects of a combination of Lactobacillus rhamnosus and inulin on mice with colitis. *Food & Function, 11*(5), 3823-3837.

Marefati, A., Pitsiladis, A., Oscarsson, E., Ilestam, N., & Bergenståhl, B. (2021). Encapsulation of Lactobacillus reuteri in W1/O/W2 double emulsions: Formulation, storage and in vitro gastro-intestinal digestion stability. *LWT, 146*, 111423.

Martins, E., Poncelet, D., Marquis, M., Davy, J., & Renard, D. (2017). Monodisperse core-shell alginate (micro)-capsules with oil core generated from droplets millifluidic. *Food Hydrocolloids, 63*, 447-456.

Meirelles, A. A. D., Costa, A. L. R., Michelon, M., Viganó, J., Carvalho, M. S., & Cunha, R. L. (2021). Microfluidic approach to produce emulsion-filled alginate microgels. *Journal of Food Engineering*, 110812.

Moghadam, H., Samimi, M., Samimi, A., & Khorram, M. (2008). Electro-spray of high viscous liquids for producing mono-sized spherical alginate beads. *Particuology, 6*(4), 271-275.

Nativel, F., Renard, D., Hached, F., Pinta, P.-G., D'Arros, C., Weiss, P., Le Visage, C., Guicheux, J., Billon-Chabaud, A., & Grimandi, G. (2018). Application of millifluidics to encapsulate. *Novel Biomaterials for Tissue Engineering, 19*, 162.

Nisisako, T., & Torii, T. (2008). Microfluidic large-scale integration on a chip for mass production of monodisperse droplets and particles. *Lab on a Chip, 8* (2), 287-293.

Nualkaekul, S., Lenton, D., Cook, M. T., Khutoryanskiy, V. V., & Charalampopoulos, D. (2012). Chitosan coated alginate beads for the survival of microencapsulated Lactobacillus plantarum in pomegranate juice. *Carbohydrate Polymers, 90* (3), 1281-1287.

Okuro, P. K., Gomes, A., Costa, A. L. R., Adame, M. A., & Cunha, R. L. (2019). Formation and stability of W/O-high internal phase emulsions (HIPEs) and derived O/W emulsions stabilized by PGPR and lecithin. *Food Research International, 122*, 252-262.

Okuro, P. K., Thomazini, M., Balieiro, J. C., Liberal, R. D., & Fávaro-Trindade, C. S. (2013). Co-encapsulation of Lactobacillus acidophilus with inulin or polydextrose in solid lipid microparticles provides protection and improves stability. *Food Research International, 53*(1), 96-103.

Pereda, M., Poncelet, D., & Renard, D. (2019). Characterization of core-shell alginate capsules. *Food Biophysics, 14*(4), 467-478.

Pitigraisorn, P., Srichaisupakit, K., Wongpadungkiat, N., & Wongsasulak, S. (2017). Encapsulation of Lactobacillus acidophilus in moist-heat-resistant multilayered microcapsules. *Journal of food Engineering, 192*, 11-18.

Quintana, G., Gerbino, E., Alves, P., Simões, P. N., Rúa, M. L., Fuciños, C., & Gomez-Zavaglia, A. (2021). Microencapsulation of Lactobacillus plantarum in W/O emulsions of okara oil and block-copolymers of poly (acrylic acid) and pluronic using microfluidic devices. *Food Research International, 140*, 110053.

Rao, A., Shiwnarain, N., & Maharaj, I. (1989). Survival of microencapsulated Bifidobacterium pseudolongum in simulated gastric and intestinal juices. *Canadian Institute of Food Science and Technology Journal, 22*(4), 345-349.

Rousseau, I., Le Cerf, D., Picton, L., Argillier, J., & Muller, G. (2004). Entrapment and release of sodium polystyrene sulfonate (SPS) from calcium alginate gel beads. *European Polymer Journal, 40*(12), 2709-2715.

Sathyabama, S., & Vijayabharathi, R. (2014). Co-encapsulation of probiotics with prebiotics on alginate matrix and its effect on viability in simulated gastric environment. *LWT-Food Science and Technology, 57*(1), 419-425.

Sciarini, L., Maldonado, F., Ribotta, P., Pérez, G., & León, A. (2009). Chemical composition and functional properties of Gleditsia triacanthos gum. *Food Hydrocolloids, 23*(2), 306-313.

Shi, L.-E., Li, Z.-H., Zhang, Z.-L., Zhang, T.-T., Yu, W.-M., Zhou, M.-L., & Tang, Z.-X. (2013). Encapsulation of Lactobacillus bulgaricus in carrageenan-locust bean gum coated milk microspheres with double layer structure. *LWT-Food Science and Technology, 54*(1), 147-151.

Silva, M. P., Tulini, F. L., Martins, E., Penning, M., Favaro-Trindade, C. S., & Poncelet, D. (2018). Comparison of extrusion and co-extrusion encapsulation techniques to protect Lactobacillus acidophilus LA3 in simulated gastrointestinal fluids. *LWT, 89*, 392-399.

Silva, M. P., Tulini, F. L., Ribas, M. M., Penning, M., Fávaro-Trindade, C. S., & Poncelet, D. (2016). Microcapsules loaded with the probiotic Lactobacillus paracasei BGP-1 produced by co-extrusion technology using alginate/shellac as wall material: Characterization and evaluation of drying processes. *Food Research International, 89*, 582-590.

Solanki, H. K., Pawar, D. D., Shah, D. A., Prajapati, V. D., Jani, G. K., Mulla, A. M., & Thakar, P. M. (2013). Development of microencapsulation delivery system for long-term preservation of probiotics as biotherapeutics agent. *BioMed Research International.*

Vagner, S., Patlazhan, S., & Serra, C. (2018). Formation of microdroplets in Newtonian and shear thinning fluids flowing in coaxial capillaries: Numerical modeling. In *Journal of Physics: Conference Series* (Vol. 946, pp. 012117): IOP Publishing.

Wohl, M. (1968). Isothermal laminar flow of non-Newtonian fluids in pipes. *Chemical Engineering*, 18-21.

Xu, C., & Xie, T. (2017). Review of microfluidic liquid–liquid extractors. *Industrial & Engineering Chemistry Research, 56*(27), 7593-7622.

Xu, J., Li, S., Tan, J., Wang, Y., & Luo, G. (2006). Controllable preparation of monodisperse O/W and W/O emulsions in the same microfluidic device. *Langmuir, 22*(19), 7943-7946.

Yoha, K. S., Nida, S., Dutta, S., Moses, J. A., & Anandharamakrishnan, C. (2021). Targeted Delivery of Probiotics: Perspectives on Research and Commercialization. *Probiotics and Antimicrobial Proteins*.

Zaeim, D., Sarabi-Jamab, M., Ghorani, B., & Kadkhodaee, R. (2019). Double layer co-encapsulation of probiotics and prebiotics by electro-hydrodynamic atomization. *LWT, 110*, 102-109.

Zaeim, D., Sarabi-Jamab, M., Ghorani, B., Kadkhodaee, R., Liu, W., & Tromp, R. H. (2020). Microencapsulation of probiotics in multi-polysaccharide microcapsules by electro-hydrodynamic atomization and incorporation into ice-cream formulation. *Food Structure, 25*, 100147.

Zhang, Z., Gu, M., You, X., Sela, D. A., Xiao, H., & McClements, D. J. (2021). Encapsulation of bifidobacterium in alginate microgels improves viability and targeted gut release. *Food Hydrocolloids, 116*, 106634.

Figures:

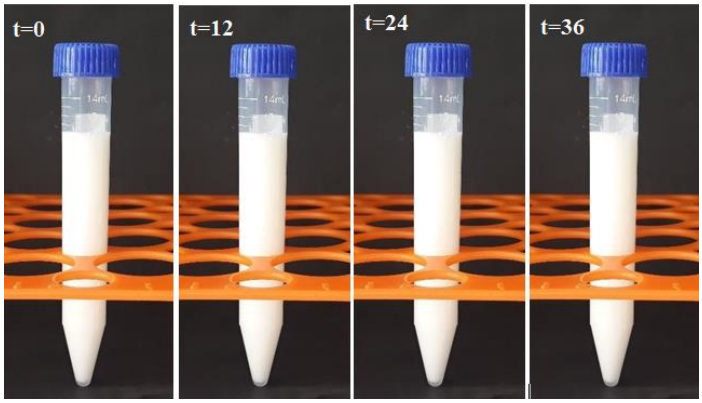

Fig. 1. Stability of W/O emulsion containing probiotics during 36 h storage time

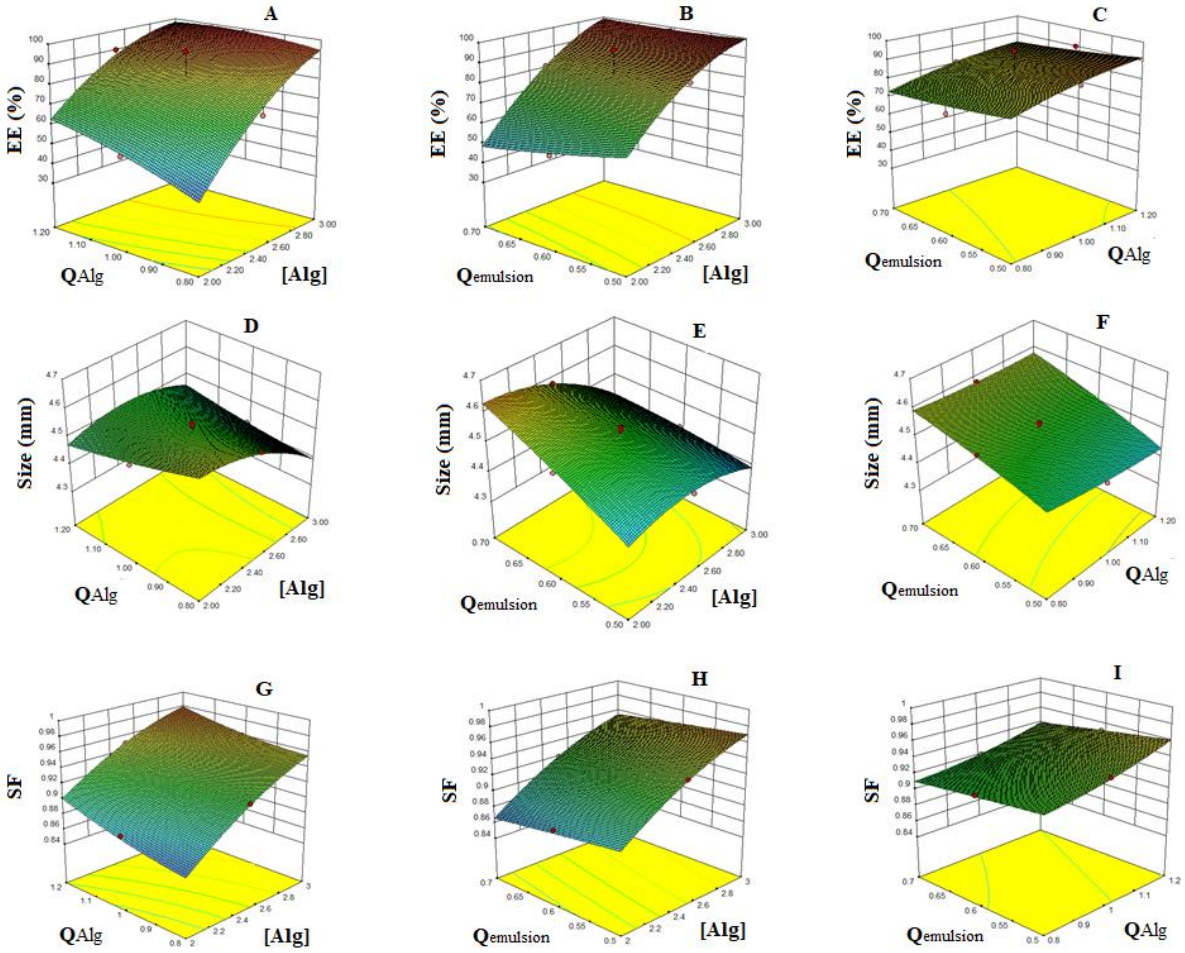

Fig. **2.** Three-dimensional plots of the response surfaces for EE (A-C), Size (D-F), and SF (G-I) as a function of interactions between concentration and flow rates of the alginate (A, D, G), alginate concentration and flow rate of emulsion (B, E, H), and flow rates of the emulsion and alginate (C, F, I).

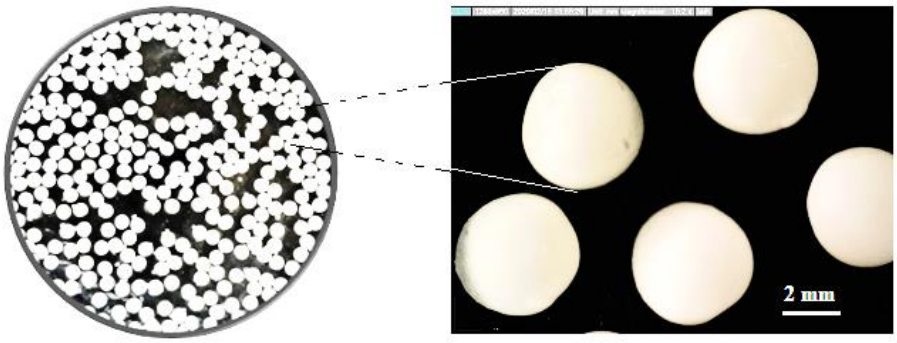

Fig 3. Digital microscopic images of the emulsion-filled millicapsule produced at the optimized conditions ([Alg]: 30 g/l, Q_{Alg}: 1.2 ml/min, $Q_{emulsion}$: 0.5 ml/min) of the millifluidic encapsulation

Tables:

Table 1. Coded and uncoded factors for RSM were ascertained from 20 experimental runs of CCD design.

Run	Uncoded variables			Coded variables		
	[Alg], (g/l)	Q_{Alg}, (ml/min)	$Q_{emulsion}$, (ml/min)	X_1	X_2	X_3
1	25	1.2	0.6	0	+1	0
2	25	1	0.6	0	0	0
3	30	1.2	0.5	+1	+1	-1
4	25	1	0.7	0	0	+1
5	25	1	0.5	0	0	-1
6	20	1.2	0.5	-1	+1	-1
7	25	1	0.6	0	0	0
8	25	1	0.6	0	0	0
9	20	1.2	0.7	-1	+1	+1
10	25	0.8	0.6	0	-1	0
11	20	0.8	0.7	-1	-1	+1
12	20	1	0.6	-1	0	0
13	30	1.2	0.7	+1	+1	+1
14	30	1	0.6	+1	0	0
15	30	0.8	0.7	+1	-1	+1
16	20	0.8	0.5	-1	-1	-1
17	25	1	0.6	0	0	0
18	25	1	0.6	0	0	0
19	30	0.8	0.5	+1	-1	-1
20	25	1	0.6	0	0	+1

Table 2. Rheological parameters of the continuous (alginate solutions) and dispersed phases (W/O emulsion) in the power-law model and viscosity at the simulated shear rate in the millifluidic tube

Phase	Power-law model				Flow rate (ml/min)	Simulated shear rate (1/s)	Viscosity at the simulated shear rate (mP.s)
	k	n	R^2	RMSE			
W/O emulsion	0.77± 0.02[d]	0.96± 0.01[a]	0.99	0.02	0.5	2.6 [h]	76.13± 0.66 [h]
					0.6	3.15 [g]	87.18± 0.84 [g]
					0.8	3.78 [g]	89.14± 0.47 [g]
Alg 20	317.6± 0.9[c]	0.72± 0.03[b]	0.99	0.31	0.8	4.42 [f]	114.61± 0.23 [f]
					1	5.44 [d]	115.82± 1.03 [f]
					1.2	6.81 [b]	118.60± 0.40 [f]
Alg 25	486.72± 1.6[b]	0.68± 0.06[c]	0.99	0.18	0.8	4.51 [f]	157.75± 1.11 [e]
					1	5.54 [d]	162.15± 1.09 [d]
					1.2	6.92 [b]	165.71± 0.59 [d]
Alg 30	1853.08± 1.07[a]	0.56± 0.02[d]	0.98	0.09	0.8	4.82 [e]	401.94± 1.47 [c]
					1	5.92 [c]	416.53± 1.91 [b]
					1.2	7.41 [a]	431.42± 1.08 [a]

Values represent means ± SD (number of test repetitions= 3).

Different letters within the same column show significant differences ($p < 0.05$).

Table 3. Second-ordered quadratic models developed for EE, size and SF

Responses	Predicted models	R^2	R^2_{adj}	covariance	Adequate precision
EE	Y_1 (EE) = 83.63- 22.06 X_1- 6.15 X_2- 3.34 X_3- 4.42 X_1X_2 + 3.25 X_1X_3 – 0.11 X_2X_3 – 7.11 X_1^2- 2.14 X_2^2+ 0.74 X_3^2	0.97	0.97	5.31	21.16
Size	Y_2 (size) = 4.52- 0.054 X_1- 0.01 X_2+ 0.06 X_3+ 0.04 X_1X_2- 0.04 X_1X_3+ 0.01 X_2X_3- 0.05 X_1^2	0.92	0.93	0.25	41.12
SF	Y_3 (SF) = 0.93+ 0.043 X_1+ 0.016 X_2- (9×10^{-3}) X_3- (3.75×10^{-3}) X_1X_2+ (1.25×10^{-3}) X_1X_3- (1.25×10^{-3}) X_2X_3- 0.01 X_1^2+ (4.54×10^{-3}) X_2^2- (4.5×10^{-4}) X_3^2	0.99	0.99	0.22	95.35

Table 4. Survival of the encapsulated probiotics in the simulated gastrointestinal fluids

Type of microorganism	Initial number of live cells after encapsulation process (Log CFU mL^{-1})	Number of live bacteria in the simulated gastric fluid (Log CFU mL^{-1})			Number of live bacteria in the simulated intestinal fluid (Log CFU mL^{-1})		
		The moment of entering the fluid	After 1 hour	After 2 hours	The moment of entering the fluid	After 1 hour	After 2 hours
Lactobacillus plantarum	9.31±0.05*^{Aa}**	8.37±0.21 ^{Bb}	8.49±0.15 ^{Ab}	7.97±0.12 ^{Ac}	7.46±0.16 ^{Ad}	7.80±0.04 ^{Ac}	7.50±0.19 ^{Ad}
Bifidobacterium animalis	9.59±0.06^{Ba}	8.72±0.12 ^{Ab}	8.24±0.23 ^{Ac}	7.39±0.09 ^{Bde}	7.17±0.15 ^{Ae}	7.26±0.16 ^{Be}	7.54±0.08 ^{Ad}

* mean ± standard deviation (n=3)
**Different capital letters in each column indicate the significant differences ($p<0.05$).
**Different small letters in each row indicate the significant differences ($p<0.05$).

Table 5. Survival of the encapsulated probiotics during storage (log CFU g^{-1})

Sampling time	Type of microorganism	
	Lactobacillus plantarum	*Bifidobacterium animalis*
After encapsulation process	9.43±0.01* Aa**	9.37±0.28 Aa
After 1 month	8.59±0.03 Ba	8.36±0.14 Bb
After 2 months	8.07±0.23 Ca	7.64±0.01 Cb
After 3 months	7.39±0.00 Db	7.61±0.12 Ca
After 4 months	7.00±0.29 Ea	7.16±0.07 Da
After 5 months	6.39±0.07 Fb	6.67±0.15 Ea
After 6 months	5.41±0.08 Ga	5.49±0.09 Fa

* mean ± standard deviation (n=3)
**Different capital letters in each column indicate the significant differences ($p<0.05$).
**Different small letters in each row indicate the significant differences ($p<0.05$).

Conflict of Interest Disclosure Statement

We wish to confirm that there are no known conflicts of interest associated with this publication and there has been no significant financial support for this work that could have influenced its outcome.

We confirm that the manuscript has been read and approved by all named authors and that there are no other persons who satisfied the criteria for authorship but are not listed. We further confirm that the order of authors listed in the manuscript has been approved by all of us.

We confirm that we have given due consideration to the protection of intellectual property associated with this work and that there are no impediments to publication, including the timing of publication, with respect to intellectual property. In so doing we confirm that we have followed the regulations of our institutions concerning intellectual property.

We understand that the Corresponding Author is the sole contact for the Editorial process (including Editorial Manager and direct communications with the office). He/she is responsible for communicating with the other authors about progress, submissions of revisions and final approval of proofs. We confirm that we have provided a current, correct email address which is accessible by the Corresponding Author and which has been configured to accept email from: (behrooz.ghorani@gmail.com) or (b.ghorani@rifst.ac.ir)

Respectfully yours,

Behrouz Ghorani

12/15/2021

Dr. Behrouz Ghorani (Corresponding author)
Associate Professor
Team Leader of Electrospinning Research Group
Department of Food Nanotechnology
Research Institute of Food Science &Technology (RIFST)
Mashhad, IRAN
Tel: +98-51-35425386
Cell: +98-915-317-3173
Fax: +98-51-35425406

A Millifluidic-assisted ionic gelation technique for encapsulation of probiotics in double-layered polysaccharide structure

Contributions of Authors

Atefeh Farahmand : Investigation, Formal Analysis, Writing – Original Draft.

Behrouz Ghorani: Concenptualization, Designing the Millifluidic Equiptment, Investigation, Validation, Visualization , Writing –Reviewing and Editting, Supervision, Technical Project Director.

Bahareh Emadzadeh: Methodology, Validation, Visualization, Formal Analysis, Writing- Reviewing and Editing, Project Administeration.

Mahboobe Sarabi-Jamab: Microbial Methodology Designer, Investigation, Formal Analysis ,Validation, Writing- Reviewing and Editing.

Maryam Emadzadeh: Formal Analysis, Funding acquisition, Project Adminesteration.

Atena Modiri : Investigation, Formnal Analysis.

Nick Tucker: Visualization, Writing-Review and Editting.